

Mechanical and thermal properties of starch films reinforced with microcellulose fibres

¹Nordin, N., ^{1,2,*}Othman, S.H., ¹Kadir Basha, R. and ^{1,2}Abdul Rashid, S.

¹Department of Process and Food Engineering, Faculty of Engineering, Universiti Putra Malaysia, 43400, UPM Serdang, Selangor, Malaysia

²Institute of Advanced Technology, Universiti Putra Malaysia, 43400, UPM Serdang, Selangor, Malaysia

Article history:

Received: 28 May 2018

Received in revised form: 12 September 2018

Accepted: 12 September 2018

Available Online: 6

November 2018

Keywords:

Food packaging,

NaOH/urea,

Mechanical,

Microcellulose fibres,

TGA

DOI:

[https://doi.org/10.26656/fr.2017.2\(6\).110](https://doi.org/10.26656/fr.2017.2(6).110)

Abstract

The use of starch as food packaging material has drawn increased attention due to its biodegradability, availability, and cost-effective. In order to improve the limitations of starch films in terms of mechanical and thermal resistance, the bio-composite concept was employed. In this work, microcellulose fibres (MCF) were incorporated into thermoplastic starch (TPS) films at various loading contents (1, 5, and 10 wt%). The MCF was prepared via NaOH/urea dissolution, followed by ultrasonication. The obtained MCF was characterized by FTIR and FESEM, and the size was in the range of 2 to 15 µm in diameter and 150 µm to hundreds of micrometres in length. The effect of the MCF addition on mechanical and thermal properties of starch films was investigated using universal testing machine and thermogravimetric analysis (TGA), respectively. Due to similar polysaccharide structures and good interfacial interactions, the tensile strength (TS) and the elongation at break (EAB) of the films increased with the addition of MCF, but only at 1 wt% loading content. Meanwhile, there was no significant improvement in the degradation temperature of the composite films, due to the presence of hemicellulose compounds that interrupted the crystallinity of the MCF. The results indicated that the MCF has the potential to be utilized as reinforcement in bio-based polymers for food packaging applications.

1. Introduction

According to European Bioplastics (2017), 8.3 billion tonnes of plastics have been produced worldwide, since the early production in the 1950s. The trend seems to increase steadily from 2015 (322 million tonnes) to 2016 (335 million tonnes) whereby in Europe, the largest application (40%) of the plastics is in the packaging sector. Packaging plays an integral part in food industry whereby it crosses different stages of the food chains, especially to package the end products. Due to that, different types of plastics such as polyethylene (PE), polypropylene (PP), and polyamide (PA), have been tailor-made to meet various purposes. The concern is that, from the total production of plastics, only 9% was recycled, 12% was incinerated and about 79% of the plastics are accumulated in the landfills (Geyer *et al.*, 2017). These kinds of plastics are continuously manufactured due to their great combination of flexibility, strength, and stability for packaging purposes. However, the growing concerns over the sustainability of the environment, depletion of the petroleum resources and demands on bio-economy and green products has led

to significant development of bio-based polymers.

Among the potential bio-based polymers, starch has been considered as a promising material for food packaging owing to its renewability, availability, cost-effective, and ecological functions (Othman, 2014). Numerous studies have testified the potential of starch to form films that are odourless, tasteless, colourless, transparent, non-toxic, and biodegradable (Mali *et al.*, 2005; Ma *et al.*, 2008; Avérous and Halley, 2009; Pelissari *et al.*, 2009; Wittaya, 2012; Sadegh-Hassani and Nafchi, 2014; Alcàzar-Alay and Meireles, 2015; Chen *et al.*, 2017; Mohamed *et al.*, 2017). In order to produce films with enhanced workability and properties, plasticizers such as glycerol and sorbitol are added into native starch under heat and shear to form thermoplastic starch (TPS) (Sanyang *et al.*, 2015). Due to granules disruption and plasticization, TPS has similar behavior as the common thermoplastic polymers. However, TPS has two main disadvantages; poor mechanical properties and low thermal stability.

The emerging technologies and the growing

*Corresponding author.

Email: s.hajar@upm.edu.my

consumer demands have stimulated the innovation in food packaging industries. Bio-based composites reinforced by cellulose fibres have been considered as a promising concept as these bio-composites possessed several desired properties such as high surface area, excellent performance, unique morphology, low density, biodegradability and renewability (Siquera *et al.*, 2010; Trache *et al.*, 2016). The potential of cellulose fibres as reinforcement have been known since decades and attracted increased interest in research and product development.

Previous studies have reported the inclusion of microcrystalline cellulose (MCC) and microfibrillated cellulose (MFC) into various polymers. For instances, MCC which generally being obtained by acid hydrolysis has been incorporated into starch (Maulida *et al.*, 2016; Coelho *et al.*, 2017), soy-protein (Li *et al.*, 2015; Liu *et al.*, 2017), agar (Shankar and Rhim, 2016), chitosan (Li *et al.*, 2012), poly (lactic) acid (Haafiz, *et al.*, 2013), poly(3hydroxybutyrate) (El-Hadi, 2013), and polyvinyl alcohol (PVA) (Ali *et al.*, 2014). It has been known for the superior stiffness which could enhance the overall performance of the polymers. Meanwhile, microfibrillated cellulose (MFC) has also gained much interest as reinforcement in composite materials. Some of the recent works include the incorporation of MFC into starch (Lendvai *et al.*, 2016; Soykeabkaew *et al.*, 2017), PLA (Suryanegara *et al.*, 2017), poly (propylene carbonate) (Qi *et al.*, 2016), and PVA (Ali *et al.*, 2014). Besides its abundance and renewability, it has an outstanding modulus, high surface area, and biocompatibility. By comparing the effectiveness of MCC and MFC as reinforcement, both have been known for the remarkable reinforcing capacity. However, MFC has a higher aspect ratio due to its long and entangled fibrils rather than the rod-like cellulose crystals of MCC. This proposed that MFC is more suitable as a matrix material and reinforcement components in various products (Jonoobi *et al.*, 2015; Abdul-Khalil *et al.*, 2017).

At present, MFC is mainly produced via two routes, mechanical processes, and controlled acid hydrolysis. Some of the mechanical treatments used are grinding, electrospinning, high-intensity ultrasonication, or wet disk mill (Jonoobi *et al.*, 2015) but these methods undoubtedly require extremely high energy cost. Meanwhile, a planned acid hydrolysis can also yield MFC but this process will involve the use of strong acids such as hydrochloric acid or sulphuric acid to hydrolyze the cellulose pulps (Mandal and Chakrabarty, 2011; Shankar *et al.*, 2015; Azrina *et al.*, 2017). These harmful chemicals must be washed repeatedly by centrifugation and this has cause troublesome and a lot of chemical

waste. Alternatively, some researchers have used the chemo-mechanical method (Jonoobi *et al.*, 2011) which used chemicals like sodium hypochlorite, acetic acid, and TEMPO-mediated oxidation prior to mechanical treatment.

Considering the use of strong acid and harmful chemicals, there is a need for a more facile and safer method. Therefore, this work presents the properties of microcellulose fibres (MCF) produced via the chemo-mechanical method using NaOH and urea, combined with ultrasonication prior to the incorporation into starch films. The properties of the produced MCF were characterized by field emission scanning electron microscopy (FESEM) analysis and Fourier transform infrared (FTIR) spectroscopy. The effects of MCF concentration on mechanical and thermal properties of the starch film were also explored.

2. Materials and methods

2.1 Preparation of microcellulose fibres (MCF)

Dried cellulose pulps were obtained by WARIS NOVE Sdn. Bhd, Malaysia. An amount of 3 g of dried cellulose pulps was added into 100 mL of 7% w/w NaOH (R&M, United Kingdom) and 12% w/w urea (R&M, United Kingdom), and stirred at room temperature using magnetic stirrer (Favorit, PLT Scientific, Malaysia) at 1,000 rpm, for 30 mins. Then, the sample was kept in the freezer (-18°C) for 16 hrs to facilitate the bonding and reactions of NaOH onto cellulose chains. Next, the content was stirred for 15 mins until dissolved then added with 1000 mL of deionized water. The mixture was then centrifuged (Hettich EBA 200, Germany) at 1008 x g for 10 minutes. Finally, the content was washed with deionized water for 6 to 7 times to remove the residue of urea and NaOH, and then underwent ultrasonication (Q500 Sonica, New York) for 5 mins at 75% amplitude. The content was kept at 4°C until further use.

2.2 Field emission scanning electron microscopy (FESEM)

The FESEM micrographs were viewed using NOVA NanoSEM 230 (FEI, United States) with an accelerating voltage of 3 kV in order to examine the morphology and surface structure of the MCF after treatment. MCF samples were dried at 50°C for 3 days and coated with gold before viewed using FESEM to avoid overcharging and any disturbance to the molecular structure.

2.3 Fourier transform infrared (FTIR) spectroscopy

The possible changes in the functional groups of the obtained MCF were determined using FTIR (Nicolet

6700 Thermo Nicolet, Thermo Scientific, United States). FTIR spectra were recorded using an infrared spectrometer in the range of 400 to 4,000 cm^{-1} .

2.4 Preparation of MCF/TPS composite films

MCF/TPS composite films were prepared using the solvent casting method. An amount of 3 g cornstarch (Cap Bintang, Malaysia) was dissolved in 100 mL of distilled water, containing glycerol (fixed at 30 wt% of TPS) and the solution was heated for 30 mins with stirring until the mixture was gelatinized. Then, the various amount of MCF (1, 5 and 10 wt% of TPS) was dispersed into the mixture and stirred for another 15 mins. Then, the film forming solution underwent ultrasonication for 5 mins at 50% amplitude prior to casting into 140 mm petri dish. The same procedure was applied for the preparation of the neat starch film. The films were dried under air-conditioned at 21°C for 48 hrs. The dried films were peeled off from the casting plate and conditioned in desiccator set at 25°C and 55% relative humidity for 48 hrs before further characterization.

2.5 Thickness and mechanical properties of MCF/TPS composite films

The film thickness was measured using a hand-held micrometer with an accuracy of 0.01 mm at five random points and the average value was determined.

Mechanical test was performed using Universal Testing Machine (Model 5566, Instron Engineering Corporation, United States). Films samples were cut into rectangular strips (100 mm x 15 mm) and the tensile strength (TS) and the elongation at break (EAB) were measured in accordance to standard method ASTM D882-02 (ASTM, 2002).

2.6 Thermogravimetric analysis (TGA)

The thermal degradation behaviour was analysed by TGA Instrument, Mettler Toledo (Model TGA/DSC 1 HT, Switzerland). An amount of 10g sample was put into aluminium pans under nitrogen flow at a rate of 25mL/min, in a temperature range from 25°C to 500°C with a heating rate of 10°C/min.

3. Results and discussion

3.1 Characterization of microcellulose fibres

Despite dissolution is a big issue for cellulose, urea and NaOH were apparent to dissolve the dried cellulose pulps. The dissolution of the dried cellulose pulps in NaOH and urea was observed to result in a change of colour of the cellulose fibres from brown to white colour after the treatment. It is deduced that the mixture of

NaOH and urea can act as a bleaching treatment for the cellulose fibres besides dissolving the cellulose fibres prior to the rupturing process via ultrasonication treatment. Zhang *et al.* (2013) were also in agreement, supporting that the NaOH acted as a swelling solvent, which penetrated the amorphous regions in the cellulose chains, leading to fibre swelling. Meanwhile, urea has been said not to have direct interactions with cellulose chains, but it helps to stabilize the NaOH/cellulose mixture (Zhou *et al.*, 2004, Luo and Wang, 2017; Wang *et al.*, 2017). In particular, the interactions between the amino group of urea with the OH^- ions of NaOH was believed to enhance the interactions between the Na^+ ions with the cellulose chains (Jiang *et al.*, 2014). Furthermore, this reaction was done at low temperature (-18°C) to facilitate the bonding between the Na^+ ion of the NaOH with the cellulose chains. It is deduced that the treatment of the cellulose fibres in NaOH and urea was able to destroy the hydrogen bonding between the cellulose molecules and subsequently open the structural chains to form a special loose structure. The loose and fully swelled structure of the cellulose fibres allows the breakup process via ultrasonication to produce smaller size of cellulose, which we called as microcellulose fibres (MCF).

To further observed the morphological structure of the obtained MCF, FESEM micrographs were taken at different magnifications to visualize the structure, homogeneity, and dimensions; presented in Figure 1a to Figure 1c.

Figures 1a – 1c show that the structure of the obtained MCF was long individual fibrils, relatively flat and entangled to each other forming a rope-like structure. At higher magnification, it can be seen that the surface of the fibres was distorted and wrinkled, in agreement with the results obtained by Luo and Wang (2017). The MCF was irregular in diameter and length, whereby the diameter was in the range of 2 to 15 μm , and the length was varied from 150 μm to several hundred micrometers. This has led to the relatively high aspect ratio of length to diameter and the non-uniformity of the size distribution.

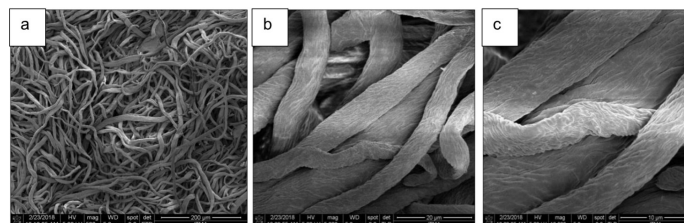


Figure 1. FESEM micrographs of microcellulose fibres at magnifications: (a) x500, (b) x5,000, and (c) x 10, 000

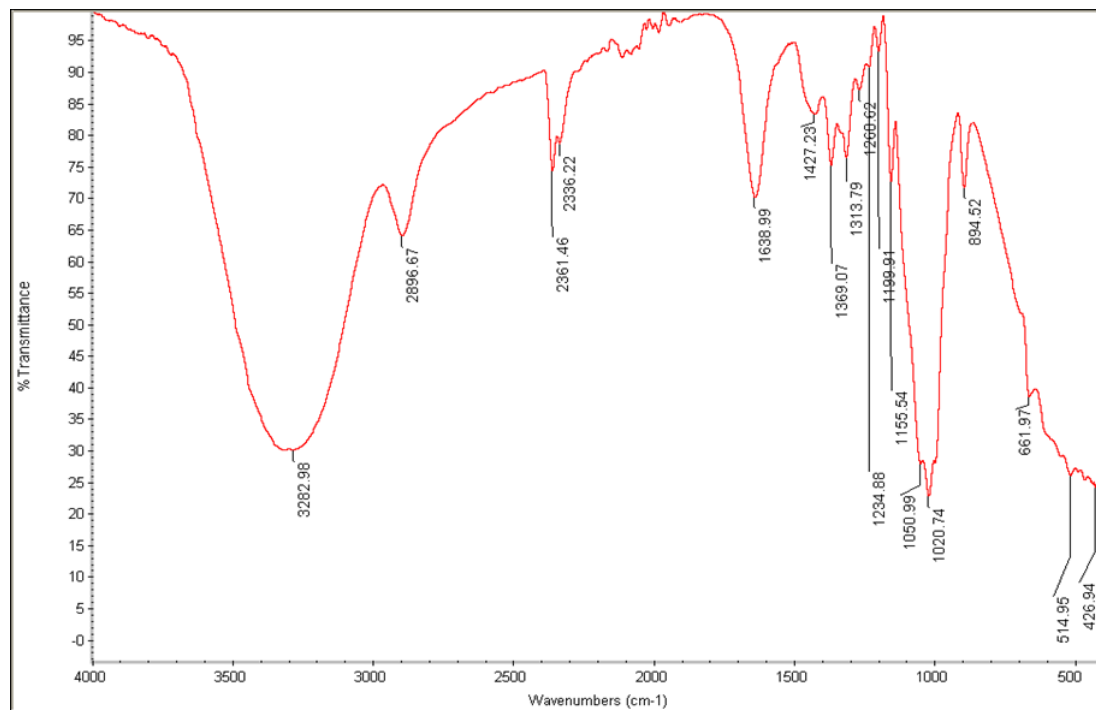


Figure 2. FTIR spectra of MCF

3.2 Characterization of MCF/TPS composite films

3.2.1 FTIR analysis

The changes in the chemical structure of the treated cellulose fibres were analysed using FTIR. The FTIR spectra in Figure 2 depicts two regions of absorbance; the first one at low wavenumbers (500-1700 cm^{-1}) and the second one at higher wavelengths (2300-3500 cm^{-1}). This observation was in line with the studies done by Moràn *et al.* (2008) and Lani *et al.* (2014). The broadband located in the range of 3600 to 3000 cm^{-1} region was attributed to the hydroxyl group O-H stretching vibrations, and the peak at 2896.67 cm^{-1} corresponded to aliphatic saturated -CH stretching vibrations. The peaks appearing at wavenumber 2330 to 2400 cm^{-1} was ascribed to triple bonds, $\text{C}\equiv\text{N}$ due to the interaction of urea and cellulose fibres. The peak presents at 1638 cm^{-1} was related to the O-H bending of adsorbed water by the cellulose. The peak at 1427 cm^{-1} was attributed to the $-\text{CH}_2$ deformation vibration that is a type of the “crystallinity band” in cellulose (Luo and Wang, 2017). The absorbance bands around 894, 1020, 1155, and 1369 cm^{-1} were associated with the C-H rocking vibrations, C-O stretching, C-O-C asymmetric valence vibration and $\text{C}-\text{H}_2$ rocking vibration, respectively, where these peaks are ascribed to cellulose form of the carbohydrates. These different bands can be seen in all spectra, regardless of the purification of the cellulose fibres (Salaberria *et al.*, 2015).

3.2.2 Thickness and mechanical properties of MCF/TPS composite films

The MCF/TPS composite films were prepared via the casting method using a different amount of MCF as a

reinforcement agent (0, 1, 5, and 10 wt% of TPS). The films obtained were flexible, transparent, smooth and easy to be peeled off. There was no significant difference in appearance between the neat starch film and the MCF/TPS composite films. Table 1 shows the thickness and tensile properties of the MCF/TPS composite films.

Table 1. Thickness and tensile properties of TPS and MCF/TPS composite films.

Types of sample	Thickness of films (mm)	Tensile strength (MPa)	Elongation at break (%)
TPS	0.078±0.07 ^a	7.49±1.87 ^a	9.18±0.81 ^a
1 wt% MCF/TPS	0.089±0.02 ^b	12.51±0.81 ^b	10.87±1.61 ^a
5 wt% MCF/TPS	0.094±0.02 ^b	8.90±0.33 ^a	2.47±0.23 ^b
10 wt% MCF/TPS	0.101±0.02 ^c	8.67±1.82 ^a	5.74±3.00 ^b

Means in the same column, with the same lower-case letters, are not significantly different ($p>0.05$).

From Table 1, it can be seen that there is a linear increment in the thickness of the composite films with the increase in the concentration of MCF added to the films. The thickness of the composite films increased mainly due to the presence of the MCF in the starch matrix. Furthermore, since the size of the MFC was relatively large, the increment of the film thickness was clearer. The data reported here confirm the association of thickness with the solid content of the films, as reported by Reddy and Rhim (2014).

As can be inferred from Table 1, the mechanical properties of TPS were greatly influenced by the concentration of the MCF. It is obvious that 1 wt% of MCF addition was able to improve the tensile strength

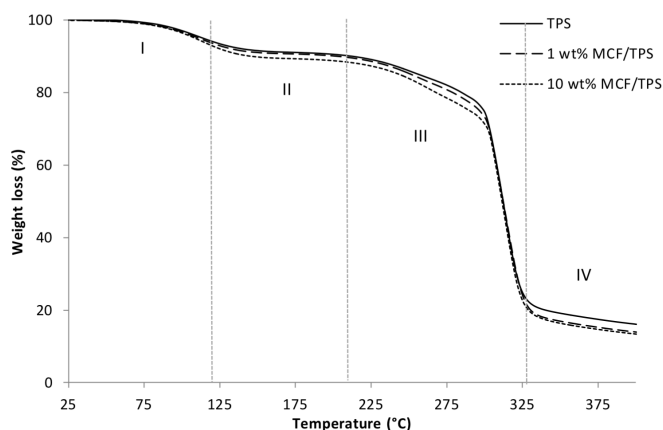


Figure 3a. TGA curves for non-reinforced TPS, 1 wt% MCF/TPS, and 10 wt% MCF/TPS composite films

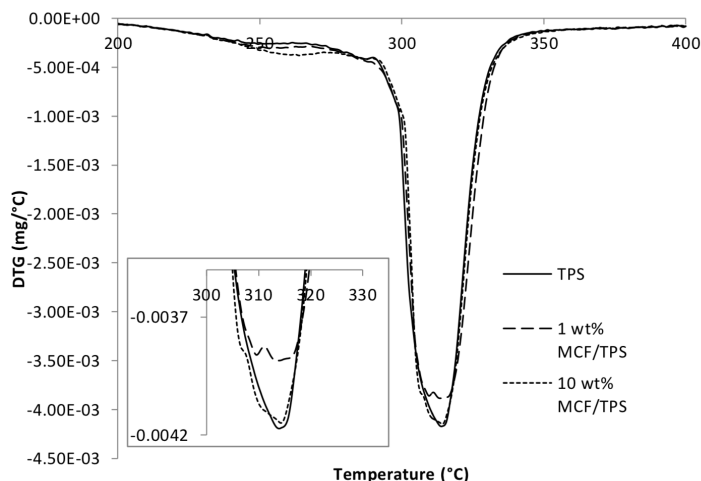


Figure 3b. DTG of non-reinforced TPS, 1 wt% MCF/TPS, and 10 wt% MCF/TPS composite films

(TS) of the films by 67%, from 7.49MPa to 12.51MPa. The elongation at break (EAB) values also shows an increment from 9.18% to 10.87% with the addition of 1 wt% of MCF. This finding was probably due to good dispersion in the film matrix and the micron size of cellulose has allowed an effective contact area with the starch matrix. Furthermore, the chemical similarities between starch and cellulose may induce a strong intermolecular interaction between the molecules through hydrogen bonding. This, in turn, was able to intensify the adhesion of the MCF to the film matrix Chen *et al.* (2017) thus increased the TS. Not only that, the effective network between the MFC and the starch improves the flexibility of the composite films which is shown by the increment in EAB by 18.4%. On the contrary, the addition of 5 wt% and 10 wt% of MCF caused a great reduction in the TS and the EAB values. The TS values obtained for 5 wt% and 10 wt% MCF/TPS films were 8.90 MPa and 8.67 MPa, respectively while the EAB values were 2.47% and 5.74%, respectively. The reduction in TS and EAB values can be explained by the fact that an excess amount of MCF formed agglomerations and non-uniform stress distribution of the MCF within the film matrix. The MCF did not form an effective network with the film matrix and thus did not act as a reinforcing agent. Savadekar and Mhaske (2012) also mentioned that an excess amount of reinforcing agent could also cause phase separation, poor particle distribution and large agglomerates, which lead to poor mechanical properties. Nevertheless, the TS values obtained were still higher than the values obtained for the neat TPS due to the good dispersion and strong interaction between the MCF and TPS matrix

Interestingly, the tensile strength of the 1 wt% MCF/TPS composite films in this study was much higher than those of MCC/starch and MFC/starch composites reported in some literature. For instance, the tensile

strength for the MCC/starch/polyester blown films was 6.5 MPa with 4% of MCC (Reis *et al.*, 2017), while 3.9 MPa for MCC/modified potato starch (Wilpiszewska and Czech, 2014). Also, Chen *et al.* (2017) found that the tensile strength for MFC/hydroxypropyl starch was in the range of 6.25 MPa to 12.54 MPa with the addition of 3 wt%, 6 wt%, and 9 wt% of MFC. In general, these results confirm the fact that micron-sized cellulose fibres produced in this work could be a reinforcing agent for bio-composite films but only to a certain limit. Meanwhile, the EAB values decreased for the 5 wt% and 10 wt% of MCF loadings which can be ascribed to the stiffness characteristics of native cellulose.

3.3 Thermal gravimetric analysis (TGA)

Table 2. Degradation temperature on maximum weight loss rate and char residue (%)

Types of sample	Degradation temperature (max DTG peak) (°C)	Weight loss at max DTG peak (%)	Char residue (%)
TPS	313	51.3	12
1 wt% MCF/TPS	309	53.5	10.1
10 wt% MCF/TPS	312	55.0	9.3

The thermogravimetric curves and the derivative thermogravimetry (DTG) curves of the neat TPS and the 1 wt% and 10 wt% of MCF/TPS composite are illustrated in Figure 3a and Figure 3b, respectively, and the relevant data are shown in Table 2. From Figure 3a, it can be seen that the neat TPS and the MCF/TPS composite films are showing similar degradation behaviour from 25°C to 500°C. Generally, the TGA curves can be divided into several phases. The initial phase occurred from 65°C to 110°C indicating evaporation of moisture from the films. There is no obvious difference could be seen among the samples due to similar contents of water as well as glycerol. Figure 3a. TGA curves for non-reinforced TPS, 1 wt% MCF/TPS, and 10 wt% MCF/TPS composite films.

The second degradation step can be observed around 120°C to 200°C due to the evaporation of glycerol (Sanyang *et al.*, 2015) together with the plasticizer compounds that were indirectly carried by water molecules (Ilyas *et al.*, 2018). This trend supports the fact that the mass loss before the onset temperature is attributed to the volatilization of both water and glycerol (Ma *et al.*, 2008). The third degradation steps were observed around 210°C to 285°C, respectively attributed to the complex process of starch degradation. This is in agreement with the report by Mathew and Dufresne (2002) and Sanyang *et al.* (2015), whereby the weight loss after the evaporation of water and plasticizer was ascribed to the dehydration of the saccharide rings and depolymerisation. The temperature range was lower than those reported in previous work, which was around 250°C-300°C (Piyada *et al.*, 2013). A possible explanation for this might be due to the difference in the amylose-amylopectin content of the starch used to prepare the films. The starch used in this study could have higher amylopectin than amylose that caused extensive branching (Rindlav-Westling *et al.*, 1998), and therefore weakens the intramolecular bonding between the starch molecules. This, in turn, leads to the mentioned complex processes occurred at a lower temperature range.

Figure 3a also shows the maximum decomposition rate occurred at around 309°C to 318°C, which is very similar for all films, reflected by the drastic weight loss. This is followed by the char residue formation in the temperature range of 325°C-500°C. The most striking observation was that the weight loss for both of the MCF/TPS composite films is higher than the neat TPS. This finding shows that the MCF did not improve the thermal resistance of starch films. Furthermore, the DTG curves in Figure 3b depicts that there is no significant difference in the maximum degradation peaks between the films. The temperature at maximum weight loss and the char yield residue (%) for all films were listed in Table 2. From Table 2, it can be seen that the char residue for the neat TPS is higher than the MCF/TPS composite films. This might be related to the presence of hemicellulose components within and between the cellulose fibres. The presence of hemicelluloses components might reduce the crystallinity of the MCF and cause the composite films to degrade faster and easier and hence, the weight loss obtained was much higher than the neat TPS film. This idea is supported by Ilyas *et al.* (2018) who speculated that the strong association between the hemicelluloses and cellulose fibrils would decrease the crystallinity of the cellulose fibrils thus accelerated the onset of the thermal degradation process.

4. Conclusion

Microcellulose fibres (MCF) was successfully prepared via the treatment of NaOH/urea, combined with ultrasonication. This facile, safe, and low-cost preparation method may be an interesting research to be explored further. The FESEM revealed that the size of the MCF was in the range of 2 to 15 µm in diameter and 150µm to hundreds of micrometers in length. The incorporation of 1 wt% MCF improved the TS and EAB values, approximately 67% and 18.4% increment, respectively. The improvement is due to the good adhesion and strong intermolecular interaction between the TPS matrix and the cellulose fibres. At 5 wt% and 10 wt% loadings of MCF, the composite films showed a decrease in TS and EAB, due to MCF agglomerations within the film matrix. On the other hand, the MCF did not show any significant thermal resistance, suggesting the presence of hemicellulose compounds that reduce the crystallinity of cellulose fibrils, leading to lower degradation temperature as compared to neat TPS films. Taken together, this work may offer significant insights for future research especially for the synthesis of microcellulose fibres and their potential use as reinforcement in bio-based polymers for food packaging applications.

Acknowledgement

This work was financially supported by the Fundamental Research Grant Scheme (FRGS), Ministry of Higher Education, Malaysia (Project no. 03-01-16-1873FR, Vote no. 5524980) .

References

- Abdul-Khalil, H.P.S., Tye, Y.Y., Saurabh, C.K., Leh, C.P., Lai, T.K., Chong, E.W.N. and Syakir, M.I. (2017). Biodegradable polymer films from seaweed polysaccharides: A review on cellulose as a reinforcement material. *Express Polymer Letters*, 11 (4), 244-265. <https://doi.org/10.3144/expresspolymlett.2017.26>
- Alcázar-Alay, S.C. and Meireles, M.A.A. (2015). Physicochemical properties. Modifications and applications of starches from different botanical sources. *Food Science and Technology (Campinas)*, 35(2), 215-236. <https://doi.org/10.1590/1678-457X.6749>
- Ali, M.E., Yong, C.K., Ching, Y.C., Chuah, C.H. and Liou, N.S. (2014). Effect of single and double stage chemically treated kenaf fibres on mechanical properties of polyvinyl alcohol film. *Bioresources*, 10(1), 822-838. <https://doi.org/10.15376/biores.10.1.822-838>

- ASTM. (2002). Standard Test Method Tensile Properties of Thin Plastic Sheeting (D882-02). Pennsylvania: ASTM International
- Avérous, L. and Halley, P.J. (2009). Biocomposites based on plasticized starch. *Biofuels, Bioproducts, and Biorefining*, 3(3), 329-343. <https://doi.org/10.1002/bbb.135>
- Azrina, Z.A.Z., Beg, M.D.H., Rosli, M.Y., Ramli, R., Junadi, N. and Alam, A.K.M.M. (2017). Spherical nanocrystalline cellulose (NCC) from oil palm empty fruit bunch pulp via ultrasound assisted hydrolysis. *Carbohydrate Polymers*, 162, 115-120. <https://doi.org/10.1016/j.carbpol.2017.01.035>
- Chen, J., Long, Z., Wang, J., Wu, M., Wang, F., Wang, B. and Lv, W. (2017). Preparation and properties of microcrystalline cellulose/hydroxypropyl starch composite films. *Cellulose*, 24(10), 4449-4459. <https://doi.org/10.1007/s10570-017-1423-6>
- Coelho, C.C.S., Cerquiera, M.A., Pereira, R.N., Pastrana, L.M., Freuras-Silva, O., Vicente, A.A. and Teixeira, J.A. (2017). Effect of moderate electric fields in the properties of starch and chitosan films reinforced with microcrystalline cellulose. *Carbohydrate Polymers*, 174, 1181-1191. <https://doi.org/10.1016/j.carbpol.2017.07.007>
- European Bioplastics (2017). Report European Bioplastics. Bioplastics Market Data 2017. Retrieved from website: <http://docs.european-bioplastics.org/>
- El-Hadi, A.M. (2013). Influence of microcrystalline cellulose fiber (MCCF) on the morphology of poly (3-hydroxybutyrate) (PHB). *Colloid and Polymer Science*, 291(3), 743-756. <https://doi.org/10.1007/s00396-012-2784-x>
- Geyer, R., Jambeck, J.R. and Law, K.L. (2017). Production, use, and fate of all plastics ever made. *Science Advances*, 3, e1700782. <https://doi.org/10.1126/sciadv.1700782>
- Haafiz, M.M., Hassan, A., Zakaria, Z., Inuwa, I.M., Islam, M.S. and Jawaid, M. (2013). Properties of polylactic acid composites reinforced with oil palm biomass microcrystalline cellulose. *Carbohydrate Polymers*, 98(1), 139-145. <https://doi.org/10.1016/j.carbpol.2013.05.069>
- Ilyas, R.A., Sapuan, S.M. and Ishak, M.R. (2018). Isolation and characterization of nanocrystalline cellulose from sugar palm fibers (*Arenga Pinnata*). *Carbohydrate Polymers*, 181, 1038-1051. <https://doi.org/10.1016/j.carbpol.2017.11.045>
- Jiang, Z., Fang, Y., Xiang, J., Lu, A., Kang, H., Huang, Y. and Zhang, L. (2014). Intermolecular interactions and 3D structure in cellulose-NaOH-urea aqueous system. *The Journal of Physical Chemistry B*, 118, 10250-10257. <https://doi.org/10.1021/jp501408e>
- Jonoobi, M., Khazaeian, A., Tahir, P.M., Asry, S.S. and Oksman, K. (2011). Characteristics of cellulose nanofibers isolated from rubberwood and empty fruit bunches of oil palm using chemo-mechanical process. *Cellulose*, 18(4), 1085-1095. <https://doi.org/10.1007/s10570-011-9546-7>
- Jonoobi, M., Oladi, R., Davoudpour, Y., Oksman, K., Dufrense, A., Hamzeh. and Davoodi, R. (2015). Different preparation methods and properties of nanostructured cellulose from various natural resources and residues: A review. *Cellulose*, 22(2), 935-969. <https://doi.org/10.1007/s10570-015-0551-0>
- Lani, N., Nagadi, N., Johari, A. and Jusoh, M. (2014). Isolation, characterization, and application of nanocellulose from oil palm empty fruit bunch fiber as nanocomposites. *Journal of Nanomaterials* (702538), 1-9. <https://doi.org/10.1155/2014/702538>
- Lendvai, L., Karger-Kocsis, J., Kmetty, Á. and Drakopoulos, S.X. (2016). Production and characterization of microfibrillated cellulose-reinforced thermoplastic starch composites. *Journal of Applied Polymer Science*, 133(2), 42397. <https://doi.org/10.1002/app.42397>
- Li, C.G., Wang, X.P., Liu, L., Chui, J.H. and Zhang, R. (2012). The effect of corn stalk microcrystalline cellulose on thermal and mechanical properties of chitosan composites. *Applied Mechanics and Materials*, 174-177, 1038-1041. <https://doi.org/10.4028/www.scientific.net/AMM.174-177.1038>
- Li, C., Luo, J., Qin, Z., Chen, H., Gao, Q. and Li, J. (2015). Mechanical and thermal properties of microcrystalline cellulose-reinforced soy-protein isolate-gelatin eco-friendly films. *RSC Advances*, 5 (70), 56518-56525. <https://doi.org/10.1039/C5RA04365D>
- Liu, W., Fei, M.E., Ban, Y., Jia, A. and Qiu, R. (2017). Preparation and evaluation of green composites from microcrystalline cellulose and a soybean-oil derivative. *Polymers*, 9(541), 1-13. <https://doi.org/10.3390/polym9100541>
- Luo, X. and Wang, X. (2017). Preparation and characterization of nanocellulose fibers from NaOH/urea pre-treatment of oil palm fibers. *Bioresources*, 12(3), 5826-5837. <https://doi.org/10.15376/biores.12.3.5826-5837>
- Ma, X., Chang, P.R. and Yu, J. (2008). Properties of biodegradable thermoplastic pea starch/carboxymethyl cellulose and pea starch/microcrystalline cellulose composites. *Carbohydrate Polymers*, 72(3), 369-375. <https://doi.org/10.1016/>

- j.carbpol.2007.09.002
- Mali, S., Sakanaka, L.S., Yamashita, F. and Grossmann, M.V.E. (2005). Water sorption and mechanical properties of cassava starch films and their relation to plasticizing effect. *Carbohydrate Polymers*, 60(3), 283-289. <https://doi.org/10.1016/j.carbpol.2005.01.003>
- Mandal, A. and Chakrabarty, D. (2011). Isolation of nanocellulose from waste sugarcane bagasse (SCB) and its characterization. *Carbohydrate Polymers*, 86 (3), 1291-1299. <https://doi.org/10.1016/j.carbpol.2011.06.030>
- Mathew, A.P. and Dufrense, A. (2002). Morphological investigation of nanocomposites from sorbitol plasticized starch and tunicin whiskers. *Biomacromolecules*, 3(3), 609-617. <https://doi.org/10.1021/bm0101769>
- Maulida, Siagian, M. and Tarigan, P. (2016). Production of starch based bioplastic from cassava peel reinforced with microcrystalline cellulose Avicel PH101 using sorbitol as plasticizer. *Journal of Physics: Conference Series*, 710, 012012.
- Mohamed, R., Mohd, M., Nurazzi, N., Siti Aisyah, M.I. and Mohd Fauzi, F. (2017). Swelling and tensile properties of starch glycerol system with various crosslinking agents. *IOP Conference Series: Materials Science and Engineering*, 223, 012059.
- Morà, J.I., Alvarez, V.A., Cyras, V.P. and Vázquez, A. (2008). Extraction of cellulose and preparation of nanocellulose from sisal fibers. *Cellulose*, 15(1), 149-159. <https://doi.org/10.1007/s10570-007-9145-9>
- Othman, S.H. (2014). Bio-nanocomposite materials for food packaging applications: Types of biopolymer and nano-sized filler. *Agriculture and Agricultural Science Procedia*, 2, 296-303. <https://doi.org/10.1016/j.aaspro.2014.11.042>
- Pelissari, F.M., Grossmann, M.V.E., Yamashita, F. and Pineda, E.A.G. (2009). Antimicrobial, mechanical, and barrier properties of cassava starch-chitosan films incorporated with oregano essential oil. *Journal of Agricultural and Food Chemistry*, 57(16), 7499-7504. <https://doi.org/10.1021/jf9002363>
- Piyada, K., Waranyou, S. and Thawien, W. (2013). Mechanical, thermal, and structural properties of rice starch films reinforced with rice starch nanocrystals. *International Food Research Journal*, 20(1), 439-449.
- Qi, X., Jing, M., Liu, Z., Dong, P., Liu, T. and Fu, Q. (2016). Microfibrillated cellulose reinforced bio-based poly (propylene carbonate) with dual responsive shape memory properties. *RSC Advances*, 6, 7560-7567. <https://doi.org/10.1039/C5RA22215J>
- Reddy, J.P. and Rhim, J.W. (2014). Characterization of bionanocomposite films prepared with agar and paper-mulberry pulp nanocellulose. *Carbohydrate Polymers*, 110, 480-488. <https://doi.org/10.1016/j.carbpol.2014.04.056>
- Reis, M.O., Olivato, J.B., Zanela, J., Yamashita, F. and Grossmann, M.V.E. (2017). Influence of microcrystalline cellulose in thermoplastic starch/polyester blown films. *Polimeros* 27(2), 129-135. <https://doi.org/10.1590/0104-1428.2338>
- Rindlav-Westling, A., Stading, M., Hermansson A.M. and Gatenholm, P. (1998). Structure, mechanical and barrier properties of amylose and amylopectin films. *Carbohydrate Polymers*, 36(2-3), 217-224. [https://doi.org/10.1016/S0144-8617\(98\)00025-3](https://doi.org/10.1016/S0144-8617(98)00025-3)
- Sadegh-Hassani, F. and Nafchi, M.A. (2014). Preparation and characterization of bionanocomposite films based on potato starch/halloysite nanoclay. *International Journal of Biological Macromolecules*, 67, 458-462. <https://doi.org/10.1016/j.ijbiomac.2014.04.009>
- Salaberria, A.M., Diaz, R.H., Labidi, J. and Fernandes, S.C.M. (2015). Role of chitin nanocrystals and nanofibers on physical, mechanical and functional properties in thermoplastic starch films. *Food Hydrocolloids*, 46, 93-102. <https://doi.org/10.1016/j.foodhyd.2014.12.016>
- Sanyang, M.L., Sapuan, S.M., Jawaid, M., Ishak, M.R. and Sahari, J. (2015). Effect of plasticizer type and concentration on tensile, thermal, and barrier properties of biodegradable films based on sugar palm (*Arenga pinnata*) starch. *Polymers*, 7(6), 1106-1124. <https://doi.org/10.3390/polym7061106>
- Savadekar, N.R. and Mhaske, S.T. (2012). Synthesis of nanocellulose fibers and effect on thermoplastic starch films. *Carbohydrate Polymers*, 89(1), 146-151. <https://doi.org/10.1016/j.carbpol.2012.02.063>
- Shankar, S., Reddy, J.P., Rhim, J.W. and Kim, H.Y. (2015). Preparation, characterization, and antimicrobial activity of chitin nanofibrils reinforced carrageenan nanocomposite films. *Carbohydrate Polymers*, 117, 468-475. <https://doi.org/10.1016/j.carbpol.2014.10.010>
- Shankar, S. and Rhim, J.-W. (2016). Preparation of nanocellulose from micro-crystalline cellulose: The effect on the performance and properties of agar-based composite films. *Carbohydrate Polymers*, 135, 18-26. <https://doi.org/10.1016/j.carbpol.2015.08.082>
- Siquera, G., Bras, J. and Dufrense, A. (2010). Cellulosic bionanocomposites: A review of preparation, properties and applications. *Polymers*, 2(4), 728-765. <https://doi.org/10.3390/polym2040728>

- Soykeabkaew, N., Tawichai, N., Thanomsilp, C. and Suwantong, O. (2017). Nanocellulose-reinforced “green” composite materials. *Walailak Journal of Science and Technology*, 14(5), 353-368.
- Trache, D., Hussin, M.H., Hui Chuin, C.T., Sabar, S., Fazita, M.R.N., Taiwo, O.F.A. and Haafiz, M.K.M. (2016). Microcrystalline cellulose: Isolation, characterization, and bio-composites application: A review. *International Journal of Biological Macromolecules*, 93(Part A), 789-804. <https://doi.org/10.1016/j.ijbiomac.2016.09.056>
- Wang, S., Sun, P., Liu, M., Lu, A. and Zhang, L. (2017). Weak interactions and their impact on cellulose dissolution in an alkali/urea aqueous system. *Physical Chemistry Chemical Physics*, 19(27), 17909-17917. <https://doi.org/10.1039/C7CP02514A>
- Wilpiszewska, K. and Czech, Z. (2014). Citric acid modified potato starch films containing microcrystalline cellulose reinforcement – properties and application. *Starch-Stärke*, 66(7-8), 660-667. <https://doi.org/10.1002/star.201300093>
- Wittaya, T. (2012). Rice Starch-Based Biodegradable Films: Properties Enhancement. In Ayman Amer Eissa (Ed). *Structure and Function of Food Engineering*. IntechOpen, Retrieved from website: <https://www.intechopen.com/books/structure-and-function-of-food-engineering/rice-starch-based-biodegradable-films-properties-enhancement>.
- Zhang, S. Wang, W., Li, F. and Yu, J. (2013). Swelling and dissolution of cellulose in NaOH aqueous solvent systems. *Cellulose Technology and Chemistry*, 67(9-10), 671-679.
- Zhou, J. Zhang, L. and Cai, J. (2004). Behaviour of cellulose in NaOH/urea aqueous solution characterized by light scattering and viscometry. *Journal of Polymer Science, Part B: Polymer Physics*, 42(2), 347-353. <https://doi.org/10.1002/polb.10636>